

**Day and night  
columnar aerosol  
properties**

D. Pérez-Ramírez et al.

# Day and night columnar aerosol properties at Granada (Spain) retrieved from sun-and star-photometry

**D. Pérez-Ramírez<sup>1,2,3</sup>, H. Lyamani<sup>1,2</sup>, F. J. Olmo<sup>1,2</sup>, D. N. Whiteman<sup>3</sup>, and L. Alados-Arboledas<sup>1,2</sup>**

<sup>1</sup>Centro Andaluz de Medio Ambiente (CEAMA), Universidad de Granada, Junta de Andalucía, Av. del Mediterráneo s/n, 18006-Granada, Spain

<sup>2</sup>Departamento de Física Aplicada, Universidad de Granada, Campus de Fuentenueva s/n, 18071-Granada, Spain

<sup>3</sup>Mesoscale Atmospheric Processes Laboratory, NASA Goddard Space Flight Center, 20771, Greenbelt-Maryland, USA

Received: 29 March 2012 – Accepted: 6 April 2012 – Published: 9 May 2012

Correspondence to: D. Pérez-Ramírez (dperez@ugr.es; daniel.perezramirez@nasa.gov)

Published by Copernicus Publications on behalf of the European Geosciences Union.

Title Page

Abstract

Introduction

Conclusions

References

Tables

Figures

⏪

⏩

◀

▶

Back

Close

Full Screen / Esc

Printer-friendly Version

Interactive Discussion



## Abstract

This work presents the first analysis of long-term day- and night-time columnar aerosol optical properties. To this end we have used a combination of sun and star photometer measurements at the city of Granada (37.16° N, 3.60° W, 680 m a.s.l.; South-East of Spain) from 2007 to 2010. For the whole study period, mean aerosol optical depth (AOD) at 440 nm ( $\pm$  standard deviation) is  $0.18 \pm 0.10$  and  $0.19 \pm 0.11$  for day- and night-time, respectively, while the mean Angström exponent ( $\alpha$ ) is  $1.0 \pm 0.4$  and  $0.9 \pm 0.4$  for day- and night-time. The ANOVA statistical tests reveal that there are no significant differences between the AOD and  $\alpha$  obtained at day-time and those obtained at night-time. Additionally, the mean day-time values of AOD and  $\alpha$  obtained during this period are within the values obtained in the surrounding AERONET stations. On the other hand, AOD presents an evident seasonal pattern characterized by large values in summer (mean values of  $0.20 \pm 0.10$  both at day- and night-time) and low values in winter (mean values of  $0.15 \pm 0.09$  at day-time and  $0.17 \pm 0.10$  at night-time). The Angström exponent presents clear seasonal pattern with low values in summer (mean values of  $0.8 \pm 0.4$  and  $0.9 \pm 0.4$  at day- and night-time) and relatively large values in winter (mean values of  $1.2 \pm 0.4$  and  $1.0 \pm 0.3$  at day- and night-time). These seasonal patterns are explained by the differences in the meteorological conditions and by the differences in the strength of aerosol sources during day and night. To take more insight about the changes in aerosol particles between day and night, the spectral difference of the Angström exponent ( $\delta\alpha$ ) as function of  $\alpha$  is also studied. This analysis reveals an increase in the fine mode radius and in the fine mode contribution to AOD during night-time, being more remarkable in summer seasons. These changes are explained by the changes in the local aerosol source emissions and meteorological conditions between day- and night-time, as well as aerosol aging processes.

### Day and night columnar aerosol properties

D. Pérez-Ramírez et al.

Title Page

Abstract

Introduction

Conclusions

References

Tables

Figures



Back

Close

Full Screen / Esc

Printer-friendly Version

Interactive Discussion



## 1 Introduction

Atmospheric aerosol is noted by the Fourth Intergovernmental Panel for Climate Change (IPCC 2007) as a key component to fully understand the climate change (Forster et al., 2007). Atmospheric aerosol particles directly affect earth's radiation budget by scattering short-wavelengths radiation and absorbing shortwave and long-wave radiation (e.g., Haywood and Shine, 1997; Forster et al., 2007). Furthermore atmospheric aerosol particles can act as cloud condensation nuclei and thus they can modify cloud droplet size and cloud albedo (Forster et al., 2007). In addition, they have effects on air quality and thus on the human health (e.g., Pope et al., 2002; Brunekreef and Forsberg, 2005; Miller et al., 2007). The IPCC 2007 also reported that anthropogenic aerosol particles (sulphate, organic carbon, black carbon or nitrate), together with natural aerosol (mineral dust or particles from volcanoes) can produce a negative radiative forcing that can be comparable but with opposite sign to the forcing induced by the increase of the concentrations of greenhouse gases (e.g., Forster et al., 2007). However, radiative forcing by atmospheric aerosol has greater uncertainties (twice its estimated value) associated with the lack of adequate information on their temporal and spatial variability (e.g., Forster et al., 2007). Therefore, it is really important to measure and characterize the aerosol optical properties in different sites for better understanding the aerosol impact at least at regional scale.

Research on the atmospheric effects of the aerosol particles has become a top priority. In this sense, several satellite programs have been developed to study long-term spectral aerosol optical depth (AOD) on a global scale (e.g., Kaufman et al., 1997; Kaufman et al., 2002; Kahn et al., 2005; Remer et al., 2005). However, satellite measurements present low temporal resolution. Surface-based passive measurements allow the study of columnar aerosol properties, and the global network AERONET (Holben et al., 1998) has been developed. But all these instrumentation acquire measurements at day-time. To date, the knowledge of columnar aerosol properties at night-time is quite limited due to the absence of continuous measurements. The study of columnar

### Day and night columnar aerosol properties

D. Pérez-Ramírez et al.

Title Page

Abstract

Introduction

Conclusions

References

Tables

Figures



Back

Close

Full Screen / Esc

Printer-friendly Version

Interactive Discussion



## Day and night columnar aerosol properties

D. Pérez-Ramírez et al.

Title Page

Abstract

Introduction

Conclusions

References

Tables

Figures

⏪

⏩

◀

▶

Back

Close

Full Screen / Esc

Printer-friendly Version

Interactive Discussion



aerosol properties at night-time will allow us to have a whole picture of the daily behavior of the atmospheric aerosol, covering the different stages in the evolution of the planetary boundary layer and pre-convection and pre-photochemistry processes that affect the atmospheric aerosol. The knowledge of AOD at night-time would also contribute to aerosol transport and chemistry models validation efforts. In addition, AOD measurements at night-time can be used as constraints for Lidar measurements (e.g., Alados-Arboledas et al., 2011). In this sense, currently some research groups are working with irradiance measurements from stars (e.g., Herber et al., 2002; Perez-Ramirez et al., 2008a; Baibakov et al., 2009) or from the moon (e.g., Berkoff et al., 2011) to obtain AOD at night-time.

To address the problem of the absence of continuous measurements of spectral AOD at night-time, this work uses the measurements of the star photometer EXCALIBUR based on a CCD camera as detector device (Perez-Ramirez et al., 2008a, b). This instrument, together with a sun photometer CIMEL, operates in the Andalusian Center for Environmental Research in the city of Granada (37.16° N, 3.60° W, 680 m a.s.l.; South-East of Spain). The star photometer EXCALIBUR is also a versatile instrument because it is able to obtain precipitable water vapor (Perez-Ramirez et al., 2012a) and has been used to estimate the sky quality in Astronomical Centers (Sanchez et al., 2007).

Atmospheric aerosol particles are constantly affected by physical and chemical processes in the atmosphere that induce changes in the optical and radiative properties of these particles. The spectral dependence of AOD is related with the sizes (types) of the predominant particles. Thus, using sun/star photometry, the possible changes in aerosol particle sizes (types) can be analyzed by means of studying the spectral dependence of AOD (e.g. O'Neill, 2001; O'Neill et al., 2003; Schuster, 2006; Gobbi et al., 2007) or by studying aerosol size distributions retrieved by inversion methods using sky radiance measurements (e.g., Dubovik and King, 2000; Dubovik et al., 2006; Olmo et al., 2006, 2008). In this study, in order to investigate the possible change in the aerosol particle sizes between day- and night-time, and due of the lack of sky radiance

measurements by the star photometer, we used the simple graphical method proposed by Gobbi et al. (2007).

The scope of this work is to analyse columnar aerosol properties obtained both at day- and night-time during the period 2007–2010 in the city of Granada. To our knowledge this study is the first work that deals with the analysis of the columnar aerosol optical properties measured both at day- and night-time. The instruments used and the experimental site are described in Sect. 2. The descriptions of the methodologies used are given in Sect. 3. Later, in Sect. 4 we present the main results, with an in depth analysis of intra-annual and seasonal evolution of columnar aerosol properties, as well as the spectral analysis of the Angström exponent, both at day- and night-time. Concluding remarks are given in Sect. 5.

## 2 Instrumentation and experimental site

Column-integrated characterization of the atmospheric aerosol at day- and night-time has been performed by means of a sun-photometer CIMEL CE-318-4 (Cimel Electronique, France), and a star-photometer EXCALIBUR (Astronómica S.L.). The CIMEL CE-318-4 makes solar extinction measurements with a  $1.2^\circ$  full field of view at 340, 380, 440, 670, 870, 940 and 1020 nm. The full-width at half-maximum (FWHM) of the interference filters are 2 nm at 340 nm, 4 nm at 380 nm and 10 nm at all the other wavelengths. More details about the CIMEL CE-318-4 can be found in e.g., Holben et al. (1998) and Alados-Arboledas et al. (2008). On other hand, the star photometer EXCALIBUR (Astronómica S.L., Spain) acquires direct star irradiance measurements at 380, 436, 500, 670, 880, 940 and 1020 nm (nominal wavelengths). The FWHM range between 7.7 and 11.2 nm for the different filters. The more innovation of this instrument is that it uses a CCD camera as detector device. Further details about this instrument can be consulted in Perez-Ramirez et al. (2008a, b).

The instruments used in this work operated in the Andalusian Centre for Environmental Research (CEAMA) located in the city of Granada ( $37.16^\circ$  N,  $3.60^\circ$  W, 680 m a.s.l.;

### Day and night columnar aerosol properties

D. Pérez-Ramírez et al.

Title Page

Abstract

Introduction

Conclusions

References

Tables

Figures



Back

Close

Full Screen / Esc

Printer-friendly Version

Interactive Discussion



South-East of Spain). Granada is a non-industrialized and medium-sized city, with a municipal population around 250 000 inhabitants and twice including its metropolitan area. The city is situated in a natural basin surrounded by mountains, with the highest hills over 3000 m a.s.l. located at the Southeast of the basin. The mediterranean-continental conditions prevailing at this site are responsible for large seasonal temperature differences, providing cool winters and hot summers. On the other hand, most of the rainfall is registered during spring and winter. The summers are usually very dry, with few rainfall events. For the past 50 yr, according to Spanish Meteorological Agency (AEMET; <http://www.aemet.es>), the mean annual rainfall in the study area is 370 mm. The relative humidity (RH) is larger in winter (with average values of 60 % and 70 % for day- and night-time, respectively) than in summer (38 % and 49 % for day- and night-time, respectively). Finally, the RH shows a clear diurnal cycle, in all the seasons, with large values at night and low values at noon.

Due to its location in the Iberian Peninsula, the study area is usually affected by air masses with different origins. African air masses usually transport large dust loads to our study area (e.g., Lyamani et al., 2005, 2006a, b; Guerrero-Rascado et al., 2009), while the air masses from Europe or the Mediterranean basin can transport large loads of anthropogenic particles (e.g., Lyamani et al., 2006b). Atlantic air masses affecting our study area are usually associated with low aerosol loads (e.g., Lyamani et al., 2010). Furthermore, the main local anthropogenic source of aerosol particles is traffic, and also domestic heating (based on fuel oil combustion) in winter (e.g., Lyamani et al., 2010, 2011; Titos et al., 2011).

### 3 Methodology

Attenuation of sun or star irradiance through earth's atmosphere follows the Beer-Bouguer-Lambert law that is given by (for an average sun/star–earth distance):

$$V(\lambda) = V_0(\lambda) \exp(-m_r \delta_{\text{atm}}(\lambda)) \quad (1)$$

## Day and night columnar aerosol properties

D. Pérez-Ramírez et al.

Title Page

Abstract

Introduction

Conclusions

References

Tables

Figures

⏪

⏩

◀

▶

Back

Close

Full Screen / Esc

Printer-friendly Version

Interactive Discussion



## Day and night columnar aerosol properties

D. Pérez-Ramírez et al.

[Title Page](#)[Abstract](#)[Introduction](#)[Conclusions](#)[References](#)[Tables](#)[Figures](#)[⏪](#)[⏩](#)[◀](#)[▶](#)[Back](#)[Close](#)[Full Screen / Esc](#)[Printer-friendly Version](#)[Interactive Discussion](#)

Where  $V(\lambda)$  is the signal measured by the photometer,  $V_0(\lambda)$  is the extraterrestrial signal (what is known as calibration constant),  $m_r$  is the optical relative air-mass and  $\delta_{\text{atm}}(\lambda)$  is the total atmospheric optical depth. The calibration of the star photometer EXCALIBUR was performed at the high mountain site of Calar Alto (37.2° N, 2.5° W, 2168 m a.s.l.), and it is made once a year (Perez-Ramirez et al., 2011). Calibration of sun photometer Cimel was performed twice a year in “Ahí de Cara” (37.1° N, 3.4° W, 2100 m a.s.l.) (Alados-Arboledas et al., 2008) following the same calibration procedures of AERONET network (Holben et al., 1998). Using Eq. (1) and sun/star photometer measurements, the aerosol optical depth (AOD( $\lambda$ )) at the selected spectral channels have been computed following the methods described in the works of Alados-Arboledas et al. (2003, 2008) and Perez-Ramirez et al. (2008a), for sun- and star-photometers, respectively. Uncertainties in AOD( $\lambda$ ) for the star photometer EXCALIBUR are 0.02 for  $\lambda < 800$  nm and 0.01 for  $\lambda > 800$  nm (Perez-Ramirez et al., 2011), and for sun photometer CIMEL are 0.02 for  $\lambda < 400$  nm and 0.01 for  $\lambda > 400$  nm (Holben et al., 1998).

Considering the Angström turbidity formula  $\text{AOD}(\lambda) = \beta \lambda^{-\alpha}$ , least-squares fits (in a log-log scale) has been applied to determine the Angström exponent  $\alpha$ . In the solar spectrum, the Angström exponent  $\alpha$  characterizes the spectral features of aerosol particles and is related to the size of the particles;  $\alpha > 1.5$  are mainly determined by the fine mode (submicron aerosols), while  $\alpha < 0.5$  are largely determined by the coarse mode (e.g., Dubovik et al., 2002; Gobbi et al., 2007). In this work, the Angström exponent,  $\alpha$  (436–880 nm), obtained at night-time is computed from AOD at 436, 667, 880 nm and the Angström exponent,  $\alpha$  (440–870 nm), obtained at day-time is calculated from AOD at 440, 670 and 870 nm.

Several authors have discussed how the spectral curvature of the Angström exponent  $\alpha$  can provide further information about the aerosol size distribution (e.g., Eck et al., 1999; O’Neill, 2001, 2003; Schuster, 2006; Gobbi et al., 2007). In this work, to take more insight about the atmospheric aerosol characteristics in our study area, we use the simple graphical method proposed by Gobbi et al. (2007). Basically, in this method, for a bimodal size distribution with different fine ( $r_f$ ) and coarse ( $r_c$ ) modal ra-

dius and fixed widths of fine and coarse modes of  $\sigma_f = 1.5\mu\text{m}$  and  $\sigma_c = 1.8\mu\text{m}$ , respectively, the difference  $\delta\alpha = \alpha(440\text{--}670\text{ nm}) - \alpha(670\text{--}870\text{ nm})$  was computed and represented versus  $\alpha(440\text{--}870\text{ nm})$ . This computation was also made taking into account different contributions of fine mode ( $\eta$ ) to AOD at 670 nm. The computations were done using the Mie theory with a fixed aerosol refractive index  $m = 1.4 - 0.001i$  (Gobbi et al., 2007). Moreover, this method assumes that the particles are spherical, which has no significant impact on the results (Gobbi et al., 2007). It is important to note that due to the large uncertainties in Angström exponent for low AOD( $\lambda$ ), this method is only applicable for AOD(670 nm) > 0.15 (Gobbi et al., 2007).

Finally, five-day backward-trajectories of the air masses affecting our study area are calculated by HYSPLIT model (Draxler and Rolph, 2003). The meteorological data used to run the model are 6-hourly GDAS (Global Data Assimilation System, ftp://www.arl.noaa.gov/pub/archives/gdas1/). The HYSPLIT model has been run twice a day at 06:00 and 12:00 UTC at fixed altitudes of 500, 1500 and 3500 m a.g.l.

## 4 Results

The data used in this work were acquired at Granada (South-East of Spain) from 2007 to 2010. Aerosol optical depths obtained by the sun-photometer were cloud-screened using the algorithm proposed by Smirnov et al. (2000). For night-time, the star photometer cloud-free data were obtained applying the algorithm proposed by Perez-Ramirez et al. (2012b). Additionally, the days and nights that present less than 2 h of measurements were eliminated from the database.

### 4.1 Temporal evolution of columnar aerosol optical depth and Angström exponent

Figure 1 shows the temporal evolutions of day-time mean values of AOD(440 nm) and night-time mean values of AOD(436 nm) acquired at Granada from 2007 to 2010. There

## Day and night columnar aerosol properties

D. Pérez-Ramírez et al.

Title Page

Abstract

Introduction

Conclusions

References

Tables

Figures

◀

▶

◀

▶

Back

Close

Full Screen / Esc

Printer-friendly Version

Interactive Discussion



are some gaps in both AOD( $\lambda$ ) data series which are due to instruments maintenance and calibrations as well as to bad meteorological conditions.

From Fig. 1, both at day- and night-time, there are variations in AOD( $\lambda$ ) which are generally of a random nature. However, these random variations are modulated by more regular longer period variations. Low values of AOD( $\lambda$ ) are more frequently found during the winter months, while large values are frequently obtained in summer months, both at day- and night-time.

Figure 2 shows the temporal evolution of day-time mean values of  $\alpha$ (440–870 nm) and night-time mean values of  $\alpha$ (436–880 nm) obtained at Granada from 2007 to 2010. As for AOD( $\lambda$ ), there is an important variability in the Angström exponent values between day-to-day and night-to-night. During the day-time,  $\alpha$ (440–870 nm) shows large values in winter and low values in summer months. However, during the night-time there are lower differences between values obtained in summer and winter months.

Table 1 present a statistical summary of day- and night-time mean values of AOD( $\lambda$ ) and  $\alpha$  for the whole study period; particularly the mean value, standard deviation (STD), median, maximum and minimum values, as well as the corresponding percentiles at 10, 25, 75 and 90 % ( $P_{10}$ ,  $P_{25}$ ,  $P_{75}$  and  $P_{90}$ ). From this table there are no significant differences between day- and night-time mean values of AOD at the same wavelength. During the day-time, AOD(440 nm) ranges from 0.02 to 0.95 with a mean value of  $0.18 \pm 0.10$ , while  $\alpha$ (440–870 nm) varies between 0.01 and 1.8 with a mean value of  $1.0 \pm 0.4$ . During the night-time, AOD(436 nm) varies from 0.02 to 0.68 with a mean value of  $0.19 \pm 0.11$ , while  $\alpha$ (436–880 nm), varies from 0.1 up to 2.1 with a mean value of  $0.9 \pm 0.4$ . The ANOVA statistical tests reveal that the mean values of AOD( $\lambda$ ) and  $\alpha$  obtained at day-time are statistically equal to those obtained at night-time. Thus there are no statistical significant differences in the sets of day- and night-time data of AOD( $\lambda$ ) and  $\alpha$ .

The standard deviations and percentiles of AOD( $\lambda$ ) and  $\alpha$  are large, both at day- and night-time, indicating the large variability of the atmospheric aerosol load and types, associated with the variability in the synoptic conditions which induce different air masses

## Day and night columnar aerosol properties

D. Pérez-Ramírez et al.

Title Page

Abstract

Introduction

Conclusions

References

Tables

Figures

◀

▶

◀

▶

Back

Close

Full Screen / Esc

Printer-friendly Version

Interactive Discussion



**Day and night  
columnar aerosol  
properties**

D. Pérez-Ramírez et al.

Title Page

Abstract

Introduction

Conclusions

References

Tables

Figures

◀◀

▶▶

◀

▶

Back

Close

Full Screen / Esc

Printer-friendly Version

Interactive Discussion



transport to our study area. Due to its location and depending on the prevailing synoptic situation, our study area can be influenced by air-mass originated in North Africa, Atlantic Ocean, Europe or Mediterranean Sea (e.g., Lyamani et al., 2006a, b, 2010). Atlantic air-mass present usually low aerosol load (Lyamani et al., 2010). The influence of Mediterranean and European air masses implies considerable loads of anthropogenic particles, with predominance of the fine particles (large values of  $\alpha$ ). On the other hand, North-African air-mass often transport large dust loads with predominance of coarse particles (low values of  $\alpha$ ) (e.g., Lyamani et al., 2004, 2005; Guerrero-Rascado et al., 2009; Valenzuela et al., 2012). Another factor that can explain this large variability of the aerosol loads and types is the variability of the meteorological conditions. Rainfall events favour the aerosol wet deposition, leading to the reduction of aerosol load. Additionally, very high values of AOD( $\lambda$ ), both at day- and night-time, can be also associated with other extreme events such as pollution or biomass burning (e.g., Alados-Arboledas et al., 2011).

For the whole study period, Fig. 3 shows the frequency distributions of AOD(440 nm) and  $\alpha$ (440–870 nm) obtained at day-time and AOD(436 nm) and  $\alpha$ (436–880 nm) obtained at night-time. Both AOD( $\lambda$ ) frequency distributions are unimodal with a strong skewness to low values of AOD( $\lambda$ ). The AOD( $\lambda$ ) modal value is 0.13 both at day- and night-time. On the other hand, the Angström exponent shows bimodal distribution both at day- and night-time. The first mode is centred at 0.55 and 0.45 with 6 % and 7 % frequencies of occurrence at day and night-time, respectively, which reflects the contribution of large particles associated with long-range transport of dust particles and with local re-suspended soil dust. The second mode is located at 1.25 and 1.05 with approximately 10 % frequencies of occurrence at day- and night-time, respectively, and evidences cases associated with a mixture of fine particles (mainly from anthropogenic origin) and coarse particles.

However, analyzing only the  $\alpha$  values does not provide clear information about the changes of fine/coarse mode to the aerosol load. To take more insight about the change of  $\alpha$  toward lower values at night-time, we used the simple graphical method proposed

by Gobbi et al. (2007). Figure 4 shows the daily mean values of the Angström exponent difference  $\delta\alpha = \alpha(440\text{--}670\text{ nm}) - \alpha(670\text{--}870\text{ nm})$  as function of  $\alpha(440\text{--}870\text{ nm})$ , and the mean values of the Angström exponent difference  $\delta\alpha = \alpha(436\text{--}670\text{ nm}) - \alpha(670\text{--}880\text{ nm})$  as function of  $\alpha(436\text{--}880\text{ nm})$  at night-time. The data that fall out of the diagram in the upper region can be explained because they have  $r_f$  lower than  $0.05\text{ }\mu\text{m}$ , while those in the bottom region can be explained by the use of a fixed refractive index (Gobbi et al., 2007).

During day-time, for AOD(670 nm) ranging from 0.15 to 0.3, most of the data present  $r_f$  values ranging from  $0.10$  to  $0.15\text{ }\mu\text{m}$ , while the fine mode fraction,  $\eta$ , reaches values up to 70 % (Fig. 4a). These large variability, together with the variation of  $\alpha(440\text{--}870\text{ nm})$  (from 0.07 to 1.63), indicate large variability in the aerosol types and sizes. At night, for AOD(670 nm) in the range 0.15–0.3 a clockwise rotation toward larger  $r_f$  (up to  $0.3\text{ }\mu\text{m}$ ) and  $\eta$  (up to 99 %) is observed. In other ranges of AOD(670 nm),  $\alpha$  is lower than 0.7 both at night- and day-time, and the clockwise rotation at night-time is observed as well. Therefore, changes in the fine mode fraction and radius between day- and night-time are observed, with increases of the fine mode fraction contribution to AOD(670 nm) and of fine mode radius at night-time. The increase of  $r_f$  at night-time could be associated with aerosol aging (e.g., Reid et al., 1998, 1999; Dubovik et al., 2002; Eck et al., 2001, 2003a, b).

## 4.2 Inter-comparison with surrounding AERONET stations

For the study period, Table 2 shows the mean AOD(440 nm) and  $\alpha(440\text{--}870)$  values obtained at 14 AERONET stations located in the Iberian Peninsula, Western Mediterranean Basin, North West Africa and Canary Island. For small urban areas in the Iberian Peninsula like Evora, Cáceres and Palencia, lower values of AOD(440 nm) than in the city of Granada are obtained. The  $\alpha(440\text{--}870\text{ nm})$  values obtained at Granada are lower than those obtained in Cáceres and Palencia. Atlantic flow advections are much more frequent in the West than in the East of the Iberian Peninsula (e.g., Querol et al., 2009), and the low aerosol load associated with these air masses (e.g., Estellés

### Day and night columnar aerosol properties

D. Pérez-Ramírez et al.

Title Page

Abstract

Introduction

Conclusions

References

Tables

Figures

◀

▶

◀

▶

Back

Close

Full Screen / Esc

Printer-friendly Version

Interactive Discussion



et al., 2007; Toledano et al., 2009) can explain the low values of AOD(440 nm) obtained at Evora, Cáceres and Palencia. Additionally, the larger impact of Saharan dust outbreaks over the South of Spain (e.g., Querol et al., 2009; Toledano et al., 2007a, 2009; Valenzuela et al., 2012) with large aerosol load and low values of the Angström exponent (e.g., Lyamani et al., 2006a, b; Toledano et al., 2007a; Cachorro et al., 2008; Guerrero-Rascado et al., 2009; Valenzuela et al., 2012) can also explain the results obtained at Granada. On other hand, although El Arenosillo is a remote station, the AOD obtained in this site is quite similar to the obtained in Granada. This can be explained by the effects of anthropogenic industrial emissions in the South-West of Spain and Saharan dust intrusions over this remote station (e.g., Toledano et al., 2007b; Prats et al., 2008; Córdoba-Jabanero et al., 2010; Bennouna et al., 2011). The stations of Valencia and Barcelona present larger values of AOD(440 nm) and  $\alpha(440\text{--}870\text{ nm})$  than those obtained at Granada station. These two sites correspond to bigger cities in Spain with considerable levels of local anthropogenic emissions. These sites are also affected by Saharan dust intrusions, but with less frequency compared with the study area which is closer to the dust sources in North Africa (e.g., Rodriguez et al., 2001; Estelles et al., 2007; Querol et al., 2009).

In other sites in the Western Mediterranean like Avignon, Ispra, Rome, Toulon and Lecce, the AOD(440 nm) and  $\alpha(440\text{--}870\text{ nm})$  values are larger than those obtained at Granada and other more polluted sites in the Iberian Peninsula such as Valencia and Barcelona. This is because these cities (Avignon, Ispra, Rome, Toulon and Lecce) are urban areas with high local anthropogenic emissions and are also quite affected by highly polluted air masses from Europe (e.g., Pace et al., 2006; Santese et al., 2008; Mazzola et al., 2010). In addition, these sites are also affected by Saharan dust intrusions (e.g., Perrone et al., 2005; Santese et al., 2008; Meloni et al., 2007; Pavese et al., 2009). It is worth noting that the station of Blida is located in North Africa and is less affected by European air masses. This station presents mean value of AOD(440 nm) of  $0.26 \pm 0.17$  and mean value of  $\alpha(440\text{--}870\text{ nm})$  around  $0.9 \pm 0.4$ . These values are explained mainly by the large influence of Saharan air masses and also by

## Day and night columnar aerosol properties

D. Pérez-Ramírez et al.

[Title Page](#)[Abstract](#)[Introduction](#)[Conclusions](#)[References](#)[Tables](#)[Figures](#)[◀](#)[▶](#)[◀](#)[▶](#)[Back](#)[Close](#)[Full Screen / Esc](#)[Printer-friendly Version](#)[Interactive Discussion](#)

the increase in the anthropogenic activity in the Magreb countries. The stations of Saada (in the North West of Africa) and La Laguna (Canary Islands) are quite affected by Saharan air masses (e.g., Alastuey et al., 2007; Garcia et al., 2009), which explain the larger values of AOD(440 nm) and lower values of  $\alpha$ (440–870 nm) obtained in these sites compared to those obtained in this study.

For the night-time, to our knowledge there are no systematic measurements of AOD( $\lambda$ ) in the surrounding areas of our station and it is not possible to make any comparison. However, AOD( $\lambda$ ) and  $\alpha$  mean values obtained in this work at night-time are quite similar to those obtained during day-time (Table 1).

### 4.3 Seasonal evolution of aerosol optical properties

To analyze the seasonal variations of aerosol optical properties, the data are grouped in four seasons: winter (January, February and December of the previous year), spring (March, April and May), summer (June, July and August) and autumn (September, October and November). For the analysed period, Table 3 presents the seasonal mean values of AOD(440 nm), AOD(436 nm),  $\alpha$ (440–870 nm) and  $\alpha$ (436–880 nm) obtained at day- and night-time at Granada.

Figure 5 shows seasonal Box-Whisker diagrams of AOD(440 nm) and  $\alpha$ (440–870 nm) obtained at day-time, and AOD(436 nm) and  $\alpha$ (436–880 nm) obtained at night-time during the analyzed period (from 2007 to 2010). In these box diagrams the mean is represented by an open square. The line segment in the box is the median. The top limit represents the 75th percentile ( $P_{75}$ ) and the bottom limit the 25th percentile ( $P_{25}$ ). The box bars are related to the 1st ( $P_1$ ) and 99th ( $P_{99}$ ) percentiles, and the crosses represent the maximum and minimum values, respectively. The lines perpendicular to the box diagrams are 1.5 the interquartile range.

Figure 5a reveals an evident seasonal pattern in AOD( $\lambda$ ), characterised by large values in summer and low ones in winter, both at day- and night-time. Spring and autumn present AOD( $\lambda$ ) values between summer and winter, both at day- and night-time. For the  $\alpha$  values, Fig. 5b also reveals a clear seasonal pattern characterized by

## Day and night columnar aerosol properties

D. Pérez-Ramírez et al.

Title Page

Abstract

Introduction

Conclusions

References

Tables

Figures

◀

▶

◀

▶

Back

Close

Full Screen / Esc

Printer-friendly Version

Interactive Discussion



low values in summer and large values in winter, both at day- and night-time. Although there are no statistical differences between day and night seasonal patterns of AOD( $\lambda$ ) and  $\alpha$ , according to the mean values of  $\alpha$  (Table 3) this parameter shows slightly more remarkable pattern at day-time than at night-time.

5 The seasonal patterns of AOD( $\lambda$ ) and  $\alpha$  can be explained by several reasons. In summer, the higher frequency of Saharan dust intrusions in our study area and the low ventilation rates of air masses in the Western-Mediterranean basin (e.g., Millan et al., 1997; Rodriguez et al., 2001; Lyamani et al., 2006a, b) can explain the large values of AOD( $\lambda$ ) and the relatively low values of the Angström exponent obtained  
10 at day- and night-time in this season. Moreover, the intense atmospheric convective dynamics prevailing in this area during summer, together with the aridity of the soil during this particular period, provide a high mineral dust (coarse particles) loading to the atmosphere from local soil. Another reason for high AOD( $\lambda$ ) values at day- and night-time in summer is the low rainfall rates, which are responsible of the aerosol load reduction. On other hand, in winter the aridity of the soil is quite reduced mainly  
15 by the rainfall and there are also less Saharan dust intrusions in our study area. In addition, the rain and clean Atlantic air masses in our study area are more frequent in this season. All this reasons can explain the low values of AOD( $\lambda$ ) and relatively high  $\alpha$  values obtained in winter both at day- and night-time.

20 In summer the convective activity is more intense at day-time than at night-time. As the convective activity ceases during the night-time, large particles can be deposited, which can lead to an increase in  $\alpha$  values and could explain the larger values of  $\alpha$  obtained at night-time in comparison with day-time. During winter, local anthropogenic emissions are the main aerosol source, which mainly inject fine particles into the atmosphere. These emissions are more active during the day-time, which explain the larger  
25 values of  $\alpha$  obtained during day-time in comparison with night-time.

Figure 6 shows the frequency distributions of day-and night-time AOD( $\lambda$ ) and  $\alpha$  for the different seasons. For AOD(440 nm) and AOD(436 nm) obtained at day- and night-time, respectively, all the distributions are unimodal with a strong skewness at lower

**Day and night  
columnar aerosol  
properties**

D. Pérez-Ramírez et al.

Title Page

Abstract

Introduction

Conclusions

References

Tables

Figures

⏪

⏩

◀

▶

Back

Close

Full Screen / Esc

Printer-friendly Version

Interactive Discussion



AOD( $\lambda$ ) values. This skewness changes to slightly larger AOD( $\lambda$ ) values in summer. In all seasons, the differences in AOD modal values between day- and night-time are negligible.

Figure 6 reveals that day- and night-time  $\alpha$  distributions present similar shape for each season. Two modes can be observed at day and night (except in winter). The first one, with modal values around 0.3–0.5, is associated with dust particles from long-range transport or from local soil. The modal  $\alpha$  values are 0.3 at day-time and 0.5 at night-time during summer and autumn, while during spring is 0.5 both at day- and night-time. These results indicate changes in coarse particles contribution between day and night (e.g. during day time there are more intense contribution of re-suspended mineral particles by the more convective activity). On the other hand, the second mode of  $\alpha$  can be observed for all the seasons, with frequencies of occurrence larger than 20 %. For the day-time, the modal values are 1.3 in spring, autumn and winter, while in summer it is 0.9. However, at night-time the modal values are 1.1, 1.1, 0.9 and 1.1 in spring, summer, autumn and winter, respectively. These differences in  $\alpha$  distributions suggest again changes in the particle sizes predominance.

To take more insight on these changes in Fig. 7 we show the plots of the Angström exponent difference ( $\delta\alpha$ ) versus  $\alpha$  at day- and night-time for each summer of the study period. Every point presented in that figure corresponds to a single measurement with sun-photometry or 30 min average measurements with star-photometry. Taking into account that only data with AOD(670 nm) > 0.15 are used, mean values of AOD(440 nm) for the summers of 2007, 2008, 2009 and 2010 are  $0.34 \pm 0.11$ ,  $0.33 \pm 0.12$ ,  $0.30 \pm 0.06$ ,  $0.32 \pm 0.10$  at day-time, while during night-time mean AOD(436 nm) values are  $0.35 \pm 0.11$ ,  $0.30 \pm 0.09$ ,  $0.28 \pm 0.07$ ,  $0.27 \pm 0.09$  for the summers of 2007, 2008, 2009 and 2010, respectively. During the day-time two patterns of data are clearly differentiated for every summer. The first one presents  $\alpha(440\text{--}870\text{ nm}) < 0.75$  and corresponds to  $\eta$  up to 30 % and  $r_f < 0.2\ \mu\text{m}$ , while  $\delta\alpha$  ranges between 0 and 0.75 for the years 2007 and 2008, and between 0 and 0.5 for the years 2009 and 2010. Backward-trajectories analysis and MODIS satellite data (graphs not shown) revealed that these data are mainly

## Day and night columnar aerosol properties

D. Pérez-Ramírez et al.

Title Page

Abstract

Introduction

Conclusions

References

Tables

Figures

◀

▶

◀

▶

Back

Close

Full Screen / Esc

Printer-friendly Version

Interactive Discussion



associated with Saharan dust intrusions. The work of Basart et al. (2009) showed that pure desert from the Sahara-Sahel measurements by sun-photometry dust particles presented  $\delta\alpha$  between  $-0.4$  and  $0.4$ ,  $\alpha < 0.3$ ,  $\eta < 40\%$  and  $r_f \sim 0.3$ . The differences between these values and those obtained in this study can be explained by the mixture of dust with local anthropogenic particles, and by the deposition of the more coarse particles during their transport to our study area. On the other hand, the second pattern is characterized by  $\alpha(440\text{--}870\text{ nm}) > 0.75$ , and most of the data present  $\eta$  ranging from 30 % to 70 % and  $r_f$  from  $0.10\text{ }\mu\text{m}$  to  $0.15\text{ }\mu\text{m}$ . These data also present  $\delta\alpha > 0$  and are associated with predominance of fine particles (e.g., Basart et al., 2009). Local anthropogenic emissions, the influence of sporadic biomass burning events in this season and anthropogenic particles transported from polluted Mediterranean and European areas can explain these values of  $\delta\alpha$  and  $\alpha(440\text{--}870\text{ nm})$  and the predominance of the fine mode particles (e.g., Lyamani et al., 2006a, b; Alados-Arboledas et al., 2011).

Although slight differences in the synoptic conditions between day and night can be found, no significant changes between day- and night-time air masses affecting our study area are expected. However, the two patterns observed at day-time data in Fig. 7 are not observed for night-time data, with  $\alpha(436\text{--}880\text{ nm})$  ranging between 0.1 and 1.3 approximately. Moreover a clockwise rotation is observed with  $\eta$ , ranging from 30 to 99 %, and  $r_f$ , ranging from 0.1 to  $0.3\text{ }\mu\text{m}$ , which imply changes in the fine mode particle characteristics between day- and night-time. As commented before in the seasonal cycle of  $\alpha$ , in summer the dryness of the ground and the intense convective processes during day can explain the large contribution of coarse particles from the ground at day-time and thus less predominance of the fine mode particles. This result is in agreement with the slightly lower values of  $\alpha$  obtained during day-time in summer (see Table 3). On the other hand, the increase of  $r_f$  at night-time can be explained by aerosol aging processes such as hygroscopic growth, coagulation and condensation. However, the hygroscopic growth is less expected in summer due to the low relative humidity obtained at surface level in the study area.

## Day and night columnar aerosol properties

D. Pérez-Ramírez et al.

Title Page

Abstract

Introduction

Conclusions

References

Tables

Figures

◀

▶

◀

▶

Back

Close

Full Screen / Esc

Printer-friendly Version

Interactive Discussion



Figure 8 shows the Angström exponent difference ( $\delta\alpha$ ) versus  $\alpha$  at day- and night-time for the winters of 2008 and 2009. In winter 2007 the star photometer was not available, while bad meteorological conditions during winter 2010 explains the lack of data.

Figure 8 shows different results between 2008 and 2009. The inter-annual variation of the air masses affecting our study area explains this difference. According to the five-day backward-trajectories analysis and MODIS satellite images, during late winter of 2008 several desert dust intrusions affect the study area (being approximately 35 % of days and nights during this winter). In the winter 2008, mean value of AOD(440 nm) is  $0.22 \pm 0.09$  at day-time, while during night-time mean value of AOD(436 nm) is  $0.21 \pm 0.06$ . From Fig. 8a, at day-time two patterns of data can be observed. The first one presents  $\delta\alpha > 0$ ,  $\alpha < 0.5$ ,  $\eta < 30\%$  and  $r_f < 0.2$ , and is mainly associated with dust particles transported from North Africa. The second one is characterised by  $\alpha > 0.75$ ,  $\eta$  up to 90 % and most data with  $r_f$  below 0.15. This last pattern is associated with a mixture of different aerosol types. The large variability of  $\delta\alpha$  in this last pattern indicates the large variability in the aerosol particle types. For night-time data, the two patterns previously mentioned are also observed and in both cases  $\eta$  values are lower than those observed at day-time. Anthropogenic emissions are more active during the day-time than during the night-time, and can explain the predominance of the fine mode particles at day-time. This result is in good agreement with the slightly larger values of  $\alpha$  observed during day-time in winter (Fig. 5b).

During the winter of 2009 (Fig. 8b) the synoptic conditions were different to those during the winter of 2008, with a lot of rain periods. The AOD(670 nm)  $> 0.15$  are observed only during the period from 18 to 26 February. For this short period, the air masses affecting our area are mainly from European continental origin. For the data presented in Fig. 8b, mean AOD(440 nm) is  $0.26 \pm 0.14$  at day-time and  $0.28 \pm 0.10$  at night-time. During the day-time,  $\eta$  ranges between 30 % and 70 %, and  $r_f$  between 0.1  $\mu\text{m}$  and 0.2  $\mu\text{m}$ . At night-time larger values of  $\eta$  and  $r_f$  are obtained. Aging processes can explain this increase of the fine mode radius; particularly the hygroscopic growth is an important

## Day and night columnar aerosol properties

D. Pérez-Ramírez et al.

[Title Page](#)[Abstract](#)[Introduction](#)[Conclusions](#)[References](#)[Tables](#)[Figures](#)[◀](#)[▶](#)[◀](#)[▶](#)[Back](#)[Close](#)[Full Screen / Esc](#)[Printer-friendly Version](#)[Interactive Discussion](#)

factor at high relative humidity for anthropogenic particles (e.g., Kotchenruther et al., 1999; Raut and Chazette, 2007; Randriamiarisoa et al., 2006; Veselovskii et al., 2009). On the other hand, from 24 to 25 February (stars symbol in Fig. 8b) there were quick and intense pollution plumes associated with air masses originated in the European continent and the Mediterranean Sea, which can explain the different patterns in  $r_f$  and  $\eta$  with those observed for the other days during this winter.

## 5 Conclusions

An analysis of day- and night-time columnar aerosol properties at Granada (South-East of Spain) is presented. This study has been possible thanks to the recent developments in star photometry combined with the well-known sun photometry technique (CIMEL instrument) To our knowledge, this is the first study of long-term night-time aerosol optical depth (AOD) and Angström exponent  $\alpha$  using passive remote sensing instrumentation.

Day- and night-time evolutions of AOD and  $\alpha$  have revealed good continuity and coherence between day- and night-time values. Moreover, the statistical analysis has shown no significant differences between columnar aerosol properties obtained at day- and night-time. For day-time values, the comparison carried out with other AERONET stations has revealed that the values obtained at Granada do not differentiate very much with those obtained in the surrounded area, in spite of the differences in synoptic conditions and aerosol sources.

A seasonal pattern for AOD has been obtained, both at day- and night-time, characterized by larger values in winter and lower values in summer. The Angström exponent also presents a seasonal pattern with lower values in summer and larger values in winter. No statistical differences between day and night AOD and  $\alpha$  have been found out. These patterns have been associated with the different soil conditions at each season, with changes in the synoptic conditions and rainfall patterns, and with the intensity of the local aerosol sources.

### Day and night columnar aerosol properties

D. Pérez-Ramírez et al.

Title Page

Abstract

Introduction

Conclusions

References

Tables

Figures

◀

▶

◀

▶

Back

Close

Full Screen / Esc

Printer-friendly Version

Interactive Discussion



## Day and night columnar aerosol properties

D. Pérez-Ramírez et al.

Title Page

Abstract

Introduction

Conclusions

References

Tables

Figures

◀

▶

◀

▶

Back

Close

Full Screen / Esc

Printer-friendly Version

Interactive Discussion



The spectral difference of the Angström exponent ( $\delta\alpha$ ) as function of  $\alpha$  has been studied, both at day-and night-time, focussing on summer and winter. During the summer season, an increase in the fine mode radius and in the fine mode contribution to AOD has been observed at night-time. It has been observed for many different air masses and aerosol loads and types. These changes have been explained by the changes in the local aerosol source emissions and meteorological conditions between day- and night-time. Moreover, the increase of the fine mode radius and AOD contribution during night-time has been also associated with aerosol aging processes. For the winter season the situation is more complex due to the more variability of synoptic conditions and aerosol sources. Nevertheless, for polluted air masses an increase in the fine mode radius and in the fine mode contribution to AOD has been also observed at night-time. However, the reduced data points obtained under these conditions make us to be careful. We would like to remark that the study of spectral variation of  $\alpha$  alone does not allow distinguishing between different aerosol aging processes. Many of such processes compete, including changes in the aerosol load due to meteorological conditions, dry/wet deposition, coagulation/condensation processes, hygroscopic growth or the injection of particles from the ground or from anthropogenic activities.

Finally, we would like to point out that the differences between day- and night-time aerosol particles are only referred to a particular site with particular conditions, and these results can not be extrapolated to any other place. In this sense, more efforts of the scientific community should be done to improve the knowledge of columnar aerosol properties at night-time.

*Acknowledgements.* This work was supported by the Spanish Ministry of Science and Technology through projects CGL2008-01330-E/CLI (Spanish Lidar Network), CGL2010-18782, CSD2007-00067 and CGL2011-13580-E/CLI; by the Andalusian Regional Government through projects P10-RNM-6299 and P08-RNM-3568; and by the EU ACTRIS project (EU INFRA-2010-1.1.16-262254). The authors would like to express their gratitude to the NASA Goddard Space Flight Center, NOAA Air Resources Laboratory and Naval Research Laboratory for the HYSPLIT model. We also thank AERONET network and especially the principal

investigators of the stations used for their efforts in establishing and maintaining the AERONET sites.

## References

- Alados-Arboledas, L., Lyamani, H., and Olmo, F. J.: Aerosol size properties at Armilla, Granada (Spain), *Q. J. Roy. Meteor. Soc.*, 129, 1395–1413, doi:10.1256/qj.01.207, 2003.
- Alados-Arboledas, L., Alcántara, A., Olmo, F. J., Martínez-Lozano, J. A., Estellés, V., Cachorro, V., Silva, A. M., Horvath, H., Gangl, M., Díaz, A., Pujadas, M., Lorente, J., Labajo, A., Sorribas, M., and Pavese, G.: Aerosol columnar properties retrieved from CIMEL radiometers during VELETA 2002, *Atmos. Environ.*, 42, 2654–2667, 2008.
- Alados-Arboledas, L., Muller, D., Guerrero-Rascado, J. L., Navas-Guzman, F., Perez-Ramirez, D., and Olmo, F. J.: Optical and microphysical properties of fresh biomass burning aerosol retrieved by Raman lidar, and star-and sun-photometry, *Geophys. Res. Lett.*, 38, L01807, doi:10.1029/2010gl045999, 2011.
- Alastuey, A., Querol, X., Castillo, S., Escudero, M., Avila, A., Cuevas, E., Torres, C., Romero, P. M., Exposito, F., García, O., Díaz, J. P., van Dingenen, R., and Putaud, J.: Characterisation of TSP and PM<sub>2.5</sub> at Izaña and Sta. Cruz de Tenerife (Canary Islands, Spain) during a Saharan dust episode (July 2002), *Atmos. Environ.*, 39, 4715–4728, 2005.
- Baibakov, K., O'Neill, N. T., Firanski, B., and Strawbridge, K.: Preliminary analysis of night-time aerosol optical depth retrievals at a rural, near-urban site in Southern Canada, in: *Current Problems in Atmospheric Radiation*, edited by: Nakajima, T. and Yamasoe, M. A., AIP Conference Proceedings, 443–446, Fox do Iguacu, Brazil, 2009.
- Basart, S., Pérez, C., Cuevas, E., Baldasano, J. M., and Gobbi, G. P.: Aerosol characterization in Northern Africa, Northeastern Atlantic, Mediterranean Basin and Middle East from direct-sun AERONET observations, *Atmos. Chem. Phys.*, 9, 8265–8282, doi:10.5194/acp-9-8265-2009, 2009.
- Bennouna, Y. S., Cachorro, V. E., Toledano, C., Berjon, A., Prats, N., Fuertes, D., Gonzalez, R., Rodrigo, R., Torres, B., and de Frutos, A. M.: Comparison of atmospheric aerosol climatologies over Southwestern Spain derived from AERONET and MODIS, *Remote Sens. Environ.*, 115, 1272–1284, doi:10.1016/j.rse.2011.01.011, 2011.

## Day and night columnar aerosol properties

D. Pérez-Ramírez et al.

Title Page

Abstract

Introduction

Conclusions

References

Tables

Figures

◀

▶

◀

▶

Back

Close

Full Screen / Esc

Printer-friendly Version

Interactive Discussion



## Day and night columnar aerosol properties

D. Pérez-Ramírez et al.

[Title Page](#)
[Abstract](#)
[Introduction](#)
[Conclusions](#)
[References](#)
[Tables](#)
[Figures](#)
[Back](#)
[Close](#)
[Full Screen / Esc](#)
[Printer-friendly Version](#)
[Interactive Discussion](#)


- Berkoff, T. A., Sorokin, M., Stone, T., Eck, T. F., Hoff, R., Welton, E., and Holben, B.: Nocturnal aerosol optical depth measurements with a small-aperture automated photometer using the moon as a light source, *J. Atmos. Oceanic Technol.*, 28, 1297–1306, doi:10.1175/JTECH-D-10-05036.1, 2011
- 5 Brunekreef, B. and Forsberg, B.: Epidemiological evidence of effects of coarse airborne particles on health, *Eur. Respir. J.*, 26, 309–318, doi:10.1183/09031936.05.00001805, 2005.
- Cachorro, V., Toledano, C., Prats, N., Sorribas, M., Mogo, S., Berjón, A., Torres, B., Rodrigo, R., de la Rosa, J., and De Frutos, A. M.: The strongest desert dust intrusion mixed with smoke over the Iberian Peninsula registered with sun photometry, *J. Geophys. Res.-Atmos.*, 113, D14S04, doi:10.1029/2007JD009582, 2008
- 10 Córdoba-Jabonero, C., Sorribas, M., Guerrero-Rascado, J. L., Adame, J. A., Hernández, Y., Lyamani, H., Cachorro, V., Gil, M., Alados-Arboledas, L., Cuevas, E., and de la Morena, B.: Synergetic monitoring of Saharan dust plumes and potential impact on surface: a case study of dust transport from Canary Islands to Iberian Peninsula, *Atmos. Chem. Phys. Discuss.*, 10, 27015–27074, doi:10.5194/acpd-10-27015-2010, 2010.
- 15 Draxler, R. R. and Rolph, G. D.: HYSPLIT (Hybrid Single-Particle Lagrangian Integrated Trajectory). Model access via NOAA ARL READY, available online: [http://ready.arl.noaa.gov/HYSPLIT\\_traj.php](http://ready.arl.noaa.gov/HYSPLIT_traj.php), 2003.
- Dubovik, O. and King, M. D.: A flexible inversion algorithm for retrieval of aerosol optical properties from sun and sky radiance measurements, *J. Geophys. Res.*, 105, 20673–20696, 2000.
- 20 Dubovik, O., Holben, B., Eck, T. F., Smirnov, A., Kaufman, Y. J., King, M. D., Tanre, D., and Slutsker, I.: Variability of absorption and optical properties of key aerosol types observed in worldwide locations, *J. Atmos. Sci.*, 59, 590–608, 2002.
- Dubovik, O., Sinyuk, A., Lapyonok, T., Holben, B. N., Mischenko, M., Yang, P., Eck, T. F., Volten, H., Muñoz, O., Veihelmann, B., van der Zande, W. J., Leon, J. F., Sorokin, M., and Slutsker, I.: Application of spheroid models to account for aerosol particle non-sphericity in remote sensing of desert dust, *J. Geophys. Res.-Atmos.*, 111, D11208, doi:10.1029/2005JD006619, 2006.
- 25 Eck, T. F., Holben, B. N., Reid, J. S., Dubovik, O., Smirnov, A., O'Neill, N. T., Slutsker, I., and Kinne, S.: Wavelength dependence of the optical depth of biomass burning, urban, and desert dust aerosols, *J. Geophys. Res.-Atmos.*, 104, 31333–31349, 1999.
- 30 Eck, T. F., Holben, B. N., Ward, D. E., Dubovik, O., Reid, J. S., Smirnov, A., Mukelabai, M. M., Hsu, N. C., O'Neill, N. T., and Slutsker, I.: Characterization of the optical properties of

**Day and night  
columnar aerosol  
properties**

D. Pérez-Ramírez et al.

Title Page

Abstract

Introduction

Conclusions

References

Tables

Figures

◀

▶

◀

▶

Back

Close

Full Screen / Esc

Printer-friendly Version

Interactive Discussion



biomass burning aerosols in Zambia during the 1997 ZIBBEE field campaign, *J. Geophys. Res.-Atmos.*, 106, 3425–3448, doi:10.1029/2000jd900555, 2001.

Eck, T. F., Holben, B. N., Reid, J. S., O'Neill, N. T., Schafer, J. S., Dubovik, O., Smirnov, A., Yamasoe, M. A., and Artaxo, P.: High aerosol optical depth biomass burning events: a comparison of optical properties for different source regions, *Geophys. Res. Lett.*, 30, 2035, doi:10.1029/2003gl017861, 2003a.

Eck, T. F., Holben, B. N., Ward, D. E., Mukelabai, M. M., Dubovik, O., Smirnov, A., Schafer, J. S., Hsu, N. C., Piketh, S. J., Queface, A., Le Roux, J., Swap, R. J., and Slutsker, I.: Variability of biomass burning aerosol optical characteristics in Southern Africa during the SAFARI 2000 dry season campaign and a comparison of single scattering albedo estimates from radiometric measurements, *J. Geophys. Res.-Atmos.*, 108, 8500, doi:10.1029/2003jd001606, 2003b.

Estelles, V., Martinez-Lozano, J. A., Utrillas, M. P., and Campanelli, M.: Columnar aerosol properties in Valencia (Spain) by ground-based sun photometry, *J. Geophys. Res.-Atmos.*, 112, D11201, doi:10.1029/2006jd008167, 2007.

Forster, P., Ramaswamy, V., Artaxo, P., Bernsten, T., Betts, R., Fahey, D. W., Haywood, J., Lean, J., Lowe, D. C., Myhre, G., Nganga, J., Prinn, R., Raga, G., Schulz, M., and Dorland, R. V.: Changes in Atmospheric Constituents and in Radiative Forcing., *Climate Change 2007: The Physical Science Basis. Contribution of Working Group I to the Fourth Assessment Report of the Intergovernmental Panel on Climate Change*, Solomon, S., D., Qin, M., Manning, Z., Chen, M., Marquis, K., Averyt, B., Tignor, M., and Miller, H. L. (eds.), 2007.

García, O. E., Díaz, A. M., Exposito, F. J., Díaz, J. P., Redondas, A., and Sasaki, T.: Aerosol radiative forcing and forcing efficiency in the UVB for regions affected by Saharan and Asian mineral dust, *J. Atmos. Sci.*, 66, 1033–1040, 2009.

Gobbi, G. P., Kaufman, Y. J., Koren, I., and Eck, T. F.: Classification of aerosol properties derived from AERONET direct sun data, *Atmos. Chem. Phys.*, 7, 453–458, doi:10.5194/acp-7-453-2007, 2007.

Guerrero-Rascado, J. L., Olmo, F. J., Avilés-Rodríguez, I., Navas-Guzmán, F., Pérez-Ramírez, D., Lyamani, H., and Alados Arboledas, L.: Extreme Saharan dust event over the southern Iberian Peninsula in september 2007: active and passive remote sensing from surface and satellite, *Atmos. Chem. Phys.*, 9, 8453–8469, doi:10.5194/acp-9-8453-2009, 2009.

Haywood, J. M. and Shine, K. P.: Multi-spectral calculations of the direct radiative forcing of tropospheric sulphate and soot aerosols using a column model, *Q. J. Roy. Meteor. Soc. A*, 123(543), 1907–1930, 1997.

## Day and night columnar aerosol properties

D. Pérez-Ramírez et al.

[Title Page](#)
[Abstract](#)
[Introduction](#)
[Conclusions](#)
[References](#)
[Tables](#)
[Figures](#)
[◀](#)
[▶](#)
[◀](#)
[▶](#)
[Back](#)
[Close](#)
[Full Screen / Esc](#)
[Printer-friendly Version](#)
[Interactive Discussion](#)


- Herber, A., Thomason, L. W., Gernandt, H., Leiterer, U., Nagel, D., Schulz, K. H., Kap-  
tur, J., Albrecht, T., and Notholt, J.: Continuous day and night aerosol optical depth ob-  
servations in the Arctic between 1991 and 1999, *J. Geophys. Res.-Atmos.*, 107, 4097,  
doi:10.1029/2001jd000536, 2002.
- 5 Holben, B. N., Eck, T. F., Slutsker, I., Tanre, D., Buis, J. P., Setzer, A., Vermote, E., Reagan, J. A.,  
Kaufman, Y. J., Nakajima, T., Lavenu, F., Jankowiak, I., and Smirnov, A.: AERONET – a  
federated instrument network and data archive for aerosol characterization, *Remote Sens.*  
*Environ.*, 66, 1–16, 1998.
- Kahn, R. A., Gaitley, B. J., Martonchik, J. V., Diner, D. J., Crean, K. A., and Holben, B.: Multiangle  
10 Imaging Spectroradiometer (MISR) global aerosol optical depth validation based on 2 years  
of coincident Aerosol Robotic Network (AERONET) observations, *J. Geophys. Res.-Atmos.*,  
110, D10s04, doi:10.1029/2004jd004706, 2005.
- Kaufman, Y. J., Wald, A. E., Remer, L. A., Gao, B. C., Li, R. R., and Flynn, L.: The MODIS  
15 2.1- $\mu\text{m}$  channel – correlation with visible reflectance for use in remote sensing of aerosol,  
*IEEE T. Geosci. Remote*, 35, 1286–1298, 1997.
- Kaufman, Y. J., Tanre, D., and Boucher, O.: A satellite view of aerosols in the climate system,  
*Nature*, 419, 215–223, doi:10.1038/nature01091, 2002.
- Kotchenruter, R. A., Hobbs, P. V., and Hegg, D. A.: Humidification factors for atmospheric  
20 aerosol off the Mid-Atlantic coast of United States, *J. Geophys. Res.-Atmos.*, 98(D12), 2239–  
2252, 1999.
- Lyamani, H., Olmo, F. J., and Alados-Arboledas, L.: Long-term changes in aerosol radiative  
properties at Armilla (Spain), *Atmos. Environ.*, 38, 5935–5943, 2004.
- Lyamani, H., Olmo, F. J., and Alados-Arboledas, L.: Saharan dust outbreak over South-  
eastern Spain as detected by sun photometer, *Atmos. Environ.*, 39, 7276–7284,  
25 doi:10.1016/j.atmosenv.2005.09.011, 2005.
- Lyamani, H., Olmo, F. J., Alcantara, A., and Alados-Arboledas, L.: Atmospheric aerosols during  
the 2003 heat wave in Southeastern Spain II: microphysical columnar properties and radi-  
ative forcing, *Atmos. Environ.*, 40, 6465–6476, doi:10.1016/j.atmosenv.2006.04.047, 2006a.
- Lyamani, H., Olmo, F. J., Alcantara, A., and Alados-Arboledas, L.: Atmospheric aerosols during  
30 the 2003 heat wave in Southeastern Spain I: spectral optical depth, *Atmos. Environ.*, 40,  
6453–6464, doi:10.1016/j.atmosenv.2006.04.048, 2006b.

**Day and night  
columnar aerosol  
properties**

D. Pérez-Ramírez et al.

Title Page

Abstract

Introduction

Conclusions

References

Tables

Figures

◀

▶

◀

▶

Back

Close

Full Screen / Esc

Printer-friendly Version

Interactive Discussion



Lyamani, H., Olmo, F. J., and Alados-Arboledas, L.: Physical and optical properties of aerosols over an urban location in Spain: seasonal and diurnal variability, *Atmos. Chem. Phys.*, 10, 239–254, doi:10.5194/acp-10-239-2010, 2010.

Lyamani, H., Olmo, F. J., Foyo, I., and Alados-Arboledas, L.: Black carbon aerosol over an urban area in South-Eastern Spain: Changes detected after the 2008 economic crisis, *Atmos. Environ.*, 45, 6423–6432, 2011.

Mazzola, M., Lanconelli, C., Lupi, A., Busetto, M., Vitale, V., and Tomasi, C.: Columnar aerosol optical properties in the Po Valley, Italy, from MFRSR data, *J. Geophys. Res.-Atmos.*, 115, D17206, doi:10.1029/2009jd013310, 2010.

Meloni, D., di Sarra, G., Biavati, G., DeLuisi, J. J., Monteleone, F., Pace, G., Piacentino, S., and Sferlazzo, D. M.: Seasonal behavior of Saharan dust events at the Mediterranean island of Lampedusa in the period 1999–2005, *Atmos. Environ.*, 41, 3041–3056, 2007.

Millan, M. M., Salvador, R., and Matilla, E.: Photo-oxidant dynamics in the Mediterranean basin in summer: Results from European research projects, *J. Geophys. Res.-Atmos.*, 102(D7), 8811–8823, 1997.

Miller, K. A., Siscovick, D. S., Sheppard, L., Shepherd, K., Sullivan, J. H., Anderson, G. L., and Kaufman, J. D.: Long-term exposure to air pollution and incidence of cardiovascular events in women, *New Engl. J. Med.*, 356, 447–458, doi:10.1056/NEJMoa054409, 2007.

O'Neill, N. T., Eck, T. F., Holben, B. N., Smirnov, A., and Dubovik, O.: Bimodal size distribution influences on the variation of Angström derivatives in spectral and optical depth space, *J. Geophys. Res.-Atmos.*, 106(D9), 9787–9806, 2001.

O'Neill, N. T., Eck, T. F., Smirnov, A., Holben, B. N., and Thulasiraman, S.: Spectral discrimination of coarse and fine mode optical depth, *J. Geophys. Res.-Atmos.*, 108, 4559, doi:10.1029/2002jd002975, 2003.

Olmo, F. J., Quirantes, A., Alcántara, A., Lyamani, H., and Alados-Arboledas, L.: Preliminary results of a non-spherical aerosol method for retrieving of the atmospheric aerosol optical properties. *J. Quant. Spectrosc. Ra.*, 100, 305–314, 2006.

Olmo, F. J., Quirantes, A., Lara, V., Lyamani, H., and Alados-Arboledas, L.: Aerosol optical properties assessed by an inversion method using the solar principal plane for non-spherical particles. *J. Quant. Spectrosc. Ra.*, 109, 1504–1516, 2008.

Pace, G., di Sarra, A., Meloni, D., Piacentino, S., and Chamard, P.: Aerosol optical properties at Lampedusa (Central Mediterranean). 1. Influence of transport and identification of different aerosol types, *Atmos. Chem. Phys.*, 6, 697–713, doi:10.5194/acp-6-697-2006, 2006.

---

**Day and night  
columnar aerosol  
properties**

---

D. Pérez-Ramírez et al.

---

[Title Page](#)[Abstract](#)[Introduction](#)[Conclusions](#)[References](#)[Tables](#)[Figures](#)[◀](#)[▶](#)[◀](#)[▶](#)[Back](#)[Close](#)[Full Screen / Esc](#)[Printer-friendly Version](#)[Interactive Discussion](#)

- Pavese, G., De Tomasi, F., Calvello, M., Esposito, F., and Perrone, M. R.: Detection of Sahara dust intrusions during mixed advection patterns over south-east Italy: a case study, *Atmos. Res.*, 92, 489–504, doi:10.1016/j.atmosres.2009.02.003, 2009.
- 5 Pérez-Ramírez, D., Aceituno, J., Ruiz, B., Olmo, F. J., and Alados-Arboledas, L.: Development and calibration of a star photometer to measure the aerosol optical depth: smoke observations at a high mountain site, *Atmos. Environ.*, 42, 2733–2738, doi:10.1016/j.atmosenv.2007.06.009, 2008a.
- Pérez-Ramírez, D., Ruiz, B., Aceituno, J., Olmo, F. J., and Alados-Arboledas, L.: Application of sun/star photometry to derive the aerosol optical depth, *Int. J. Remote Sens.*, 29, 5113–5132, doi:10.1080/01431160802036425, 2008b.
- 10 Pérez-Ramírez, D., Lyamani, H., Olmo, F. J., and Alados-Arboledas, L.: Improvements in star photometry for aerosol characterizations, *J. Aerosol Sci.*, 42, 737–745, 2011.
- Pérez-Ramírez, D., Navas-Guzman, F., Lyamani, H., Fernandez-Galvez, J., Olmo, F. J., and Alados-Arboledas, L.: Retrievals of precipitable water vapor using star photometry: assessment with Raman lidar and link to sun photometry, *J. Geophys. Res.*, 117, D05202, doi:10.1029/2011JD016450, 2012a.
- 15 Pérez-Ramírez, D., Lyamani, H., Olmo, F. J., Whiteman, D. N., Navas-Guzman, F., and Alados-Arboledas, L.: Cloud screening and quality control algorithm for star photometer data: assessment with lidar measurements and with all-sky-images, *Atmos. Meas. Tech. Discuss.*, 5, 1657–1693, doi:10.5194/amtd-5-1657-2012, 2012b.
- Perrone, M. R., Santese, M., Tafuro, A. M., Holben, B., and Smirnov, A.: Aerosol load characterization over South-East Italy for one year of AERONET sun-photometer measurements, *Atmos. Res.*, 75, 111–133, doi:10.1016/j.atmosres.2004.12.003, 2005.
- 20 Pope, C. A., Burnett, R. T., Thun, M. J., Calle, E. E., Krewski, D., Ito, K., and Thurston, G. D.: Lung cancer, cardiopulmonary mortality, and long-term exposure to fine particulate air pollution, *J. Am. Med. Assoc.*, 287, 1132–1141, doi:10.1001/jama.287.9.1132, 2002.
- Prats, N., Cachorro, V. E., Sorribas, M., Mogo, S., Berjon, A., Toledano, C., de Frutos, A. M., de la Rosa, J., Laulainen, N., and de la Morena, B. A.: Columnar aerosol optical properties during “El Arenosillo 2004 summer campaign”, *Atmos. Environ.*, 42, 2643–2653, doi:10.1016/j.atmosenv.2007.07.041, 2008.
- 30 Querol, X., Pey, J., Pandolfi, M., Alastuey, A., Cusack, M., Perez, N., Moreno, T., Viana, M., Mihalopoulos, N., Kallos, G., and Kleanthous, S.: African dust contributions to mean ambi-

**Day and night  
columnar aerosol  
properties**

D. Pérez-Ramírez et al.

Title Page

Abstract

Introduction

Conclusions

References

Tables

Figures

◀

▶

◀

▶

Back

Close

Full Screen / Esc

Printer-friendly Version

Interactive Discussion



ent PM(10) mass-levels across the Mediterranean basin, *Atmos. Environ.*, 43, 4266–4277, doi:10.1016/j.atmosenv.2009.06.013, 2009.

Randriamiarisoa, H., Chazette, P., Couvert, P., Sanak, J., and Mégie, G.: Relative humidity impact on aerosol parameters in a Paris suburban area, *Atmos. Chem. Phys.*, 6, 1389–1407, doi:10.5194/acp-6-1389-2006, 2006.

Raut, J.-C. and Chazette, P.: Retrieval of aerosol complex refractive index from a synergy between lidar, sunphotometer and in situ measurements during LISAIR experiment, *Atmos. Chem. Phys.*, 7, 2797–2815, doi:10.5194/acp-7-2797-2007, 2007.

Reid, J. S., Hobbs, P. V., Ferek, R. J., Blake, D. R., Martins, J. V., Dunlap, M. R., and Liousse, C.: Physical, chemical, and optical properties of regional hazes dominated by smoke in Brazil, *J. Geophys. Res.-Atmos.*, 103, 32059–32080, 1998.

Reid, J. S., Eck, T. F., Christopher, S. A., Hobbs, P. V., and Holben, B.: Use of the Angstrom exponent to estimate the variability of optical and physical properties of aging smoke particles in Brazil, *J. Geophys. Res.-Atmos.*, 104, 27473–27489, doi:10.1029/1999jd900833, 1999.

Remer, L. A., Kaufman, Y. J., Tanre, D., Mattoo, S., Chu, D. A., Martins, J. V., Li, R. R., Ichoku, C., Levy, R. C., Kleidman, R. G., Eck, T. F., Vermote, E., and Holben, B. N.: The MODIS aerosol algorithm, products, and validation, *J. Atmos. Sci.*, 62, 947–973, 2005.

Rodriguez, S., Querol, X., Alastuey, A., Kallos, G., and Kakaliagou, O.: Saharan dust contributions to PM<sub>10</sub> and TSP levels in Southern and Eastern Spain, *Atmos. Environ.*, 35, 2433–2447, doi:10.1016/s1352-2310(00)00496-9, 2001.

Sanchez, S. F., Aceituno, J., Thiele, U., Perez-Ramirez, D., and Alves, J.: The night sky at the Calar Alto observatory, *Publ. Astron. Soc. Pac.*, 119, 1186–1200, doi:10.1086/522378, 2007.

Santese, M., De Tomasi, F., and Perrone, M. R.: Advection patterns and aerosol optical and microphysical properties by AERONET over south-east Italy in the central Mediterranean, *Atmos. Chem. Phys.*, 8, 1881–1896, doi:10.5194/acp-8-1881-2008, 2008.

Schuster, G. L., Dubovik, O., and Holben, B. N.: Angström exponent and bimodal aerosol size distributions, *J. Geophys. Res.*, 111, D07207, doi:10.1029/2005JD006328, 2006.

Smirnov A., Holben, B. N., Eck, T. F., Dubovik, O., and Slutsker, I.: Cloud screening and quality control algorithms for the AERONET data base, *Remote Sens. Environ.*, 73, 337–349, 2000.

Titos, G., Foyo-Moreno, I., Lyamani, H., Querol, X., Alastuey, A., and Alados-Arboledas, L.: Optical properties and chemical composition of aerosol particles at an urban location: an es-

5 timation of the aerosol mass scattering and absorption efficiencies, *J. Geophys. Res.-Atmos.*, 117, D04206, doi:10.1029/2011JD016671.

Toledano, C., Cachorro, V. E., de Frutos, A. M., Sorribas, M., Prats, N., and de la Morena, B.: Inventory of African desert dust events over the Southwestern Iberian Peninsula in 2000–2005 with an AERONET Cimel sun photometer, *J. Geophys. Res.-Atmos.*, 112, D21201, doi:10.1029/2006JD008307, 2007a.

Toledano, C., Cachorro, V. E., Berjon, A., de Frutos, A. M., Sorribas, M., de la Morena, B. A., and Goloub, P.: Aerosol optical depth and Angstrom exponent climatology at El Arenosillo AERONET site (Huelva, Spain), *Q. J. Roy. Meteor. Soc.*, 133, 795–807, doi:10.1002/qj.54, 2007b.

Toledano, C., Cachorro, V. E., De Frutos, A. M., Torres, B., Berjón, A., Sorribas, M., and Stone, R. S.: Airmass classification and analysis of aerosol types at El Arenosillo (Spain), *J. Appl. Meteorol. Climatol.*, 48, 962–981, 2009.

Valenzuela, A., Olmo, F. J., Lyamani, H., Antón, M., Quirantes, A., and Alados-Arboledas, L.: Analysis of the columnar radiative properties retrieved during African desert dust events over Granada (2005–2010) using principal plane sky radiances and spheroids retrieval procedure, *Atmos. Res.*, 105, 292–301, doi:10.1016/j.atmosres.2011.11.005, 2012.

Veselovskii, I., Whiteman, D., Kolgotin, A., Andrews, E., and Korenskii, M.: Demonstration of aerosol property profiling by multiwavelength lidar under varying relative humidity conditions. *J. Atmos. Oceanic Technol.*, doi:10.1175/2009JTECHA1254.1, 2009.

## Day and night columnar aerosol properties

D. Pérez-Ramírez et al.

Title Page

Abstract

Introduction

Conclusions

References

Tables

Figures

◀

▶

◀

▶

Back

Close

Full Screen / Esc

Printer-friendly Version

Interactive Discussion



## Day and night columnar aerosol properties

D. Pérez-Ramírez et al.

**Table 1.** Day and night time spectral aerosol optical depth  $AOD(\lambda)$  and Angström exponent  $\alpha$  statistics for the 4-yr data series in the city of Granada; STD is the standard deviation;  $P10$ ,  $P25$ ,  $P75$  and  $P90$  are the corresponding percentiles at 10, 25, 75 and 90 %.

Parameter	Aerosol Optical Depth (AOD) at different wavelengths (nm)										Angström exponent	
	380	380	440	436	670	670	870	880	1020	1020	$\alpha$ (440–870)	$\alpha$ (436–880)
Wavelength (nm)	380	380	440	436	670	670	870	880	1020	1020	$\alpha$ (440–870)	$\alpha$ (436–880)
Time period	Day	Night	Day	Night	Day	Night	Day	Night	Day	Night	Day	Night
Mean	0.21	0.21	0.18	0.19	0.12	0.13	0.10	0.10	0.09	0.09	1.0	0.9
STD	0.11	0.13	0.10	0.11	0.08	0.09	0.08	0.08	0.08	0.07	0.4	0.4
$P25$	0.14	0.13	0.11	0.11	0.07	0.07	0.05	0.05	0.04	0.05	0.6	0.7
$P75$	0.26	0.27	0.22	0.24	0.14	0.16	0.12	0.13	0.10	0.11	1.3	1.2
$P10$	0.10	0.09	0.08	0.07	0.05	0.05	0.04	0.03	0.03	0.03	0.4	0.4
$P90$	0.34	0.38	0.29	0.32	0.22	0.24	0.20	0.19	0.20	0.17	1.5	1.4
Minimum	0.03	0.02	0.02	0.02	0.01	0.02	0.01	0.01	0.01	0.01	0.01	0.1
Maximum	1.07	0.90	0.95	0.68	0.94	0.63	0.91	0.62	0.90	0.59	1.8	2.1
Median	0.19	0.19	0.16	0.17	0.10	0.10	0.08	0.08	0.07	0.07	1.0	1.0

Title Page

Abstract

Introduction

Conclusions

References

Tables

Figures

◀

▶

◀

▶

Back

Close

Full Screen / Esc

Printer-friendly Version

Interactive Discussion



## Day and night columnar aerosol properties

D. Pérez-Ramírez et al.

**Table 2.** Mean values of aerosol optical depths at 440 nm and  $\alpha(440\text{--}870\text{ nm})$  obtained during the period 2007–2010 at 14 AERONET stations. A brief description of each AERONET site is also included. The stations are defined as Desert areas (D), Remote (R), Urban sites (U) and Costal areas (C).

AERONET site	Coordinates	Class	Dataset	AOD(440 nm)	$\alpha(440\text{--}870)$
Iberian Peninsula					
El Aeronosillo	37.1° N, 6.7° W, 0 m a.s.l.	R/C	963	0.17 ± 0.12	1.0 ± 0.4
Cáceres	39.5° N, 6.3° W, 347 m a.s.l.	U	792	0.14 ± 0.09	1.3 ± 0.4
Evora	38.6° N, 7.9° W, 293 m a.s.l.	U	1097	0.15 ± 0.12	1.1 ± 0.5
Palencia	42.0° N, 4.5° W, 750 m a.s.l.	U	788	0.14 ± 0.12	1.3 ± 0.5
Valencia	39.5° N, 0.4° W, 30 m a.s.l.	UC	916	0.21 ± 0.14	1.1 ± 0.4
Barcelona	41.4° N, 2.1° E, 125 m a.s.l.	UC	1077	0.22 ± 0.13	1.3 ± 0.3
Western Mediterranean Basin					
Avignon	43.9° N, 4.9° E, 32 m a.s.l.	U	1108	0.20 ± 0.13	1.4 ± 0.4
Toulon	43.1° N, 6.0° E, 50 m a.s.l.	UC	1146	0.20 ± 0.14	1.3 ± 0.5
Roma	41.8° N, 12.6° E, 130 m a.s.l.	U	949	0.24 ± 0.13	1.2 ± 0.4
Ispra	45.8° N, 8.6° E, 235 m a.s.l.	U	806	0.29 ± 0.23	1.4 ± 0.3
Lecce	40.3° N, 18.1° E, 30 m a.s.l.	UC	875	0.24 ± 0.14	1.2 ± 0.5
Blida	36.5° N, 2.9° E, 230 m a.s.l.	UC	1048	0.26 ± 0.17	0.9 ± 0.4
North-West Africa and Canary Islands					
Saada	31.6° N, 8.2° W, 420 m a.s.l.	D	1216	0.26 ± 0.17	0.7 ± 0.4
La Laguna	28.5° N, 16.3° E, 568 m a.s.l.	UC	837	0.17 ± 0.16	0.6 ± 0.3

[Title Page](#)
[Abstract](#)
[Introduction](#)
[Conclusions](#)
[References](#)
[Tables](#)
[Figures](#)
[⏪](#)
[⏩](#)
[◀](#)
[▶](#)
[Back](#)
[Close](#)
[Full Screen / Esc](#)
[Printer-friendly Version](#)
[Interactive Discussion](#)


## Day and night columnar aerosol properties

D. Pérez-Ramírez et al.

Title Page

Abstract

Introduction

Conclusions

References

Tables

Figures

◀

▶

◀

▶

Back

Close

Full Screen / Esc

Printer-friendly Version

Interactive Discussion



**Table 3.** Seasonal mean values and standard deviations of AOD( $\lambda$ ) and Angström exponent  $\alpha$ , obtained at night and day time at Granada.

Parameter		Mean values and standard deviations			
		Spring	Summer	Autumn	Winter
AOD(440 nm)	Day	$0.18 \pm 0.08$	$0.20 \pm 0.10$	$0.15 \pm 0.10$	$0.15 \pm 0.10$
AOD(436 nm)	Night	$0.16 \pm 0.08$	$0.20 \pm 0.11$	$0.15 \pm 0.11$	$0.17 \pm 0.09$
$\alpha(440\text{--}870\text{ nm})$	Day	$1.1 \pm 0.4$	$0.8 \pm 0.4$	$1.0 \pm 0.4$	$1.2 \pm 0.4$
$\alpha(436\text{--}880\text{ nm})$	Night	$1.1 \pm 0.4$	$0.9 \pm 0.4$	$0.9 \pm 0.4$	$1.0 \pm 0.3$

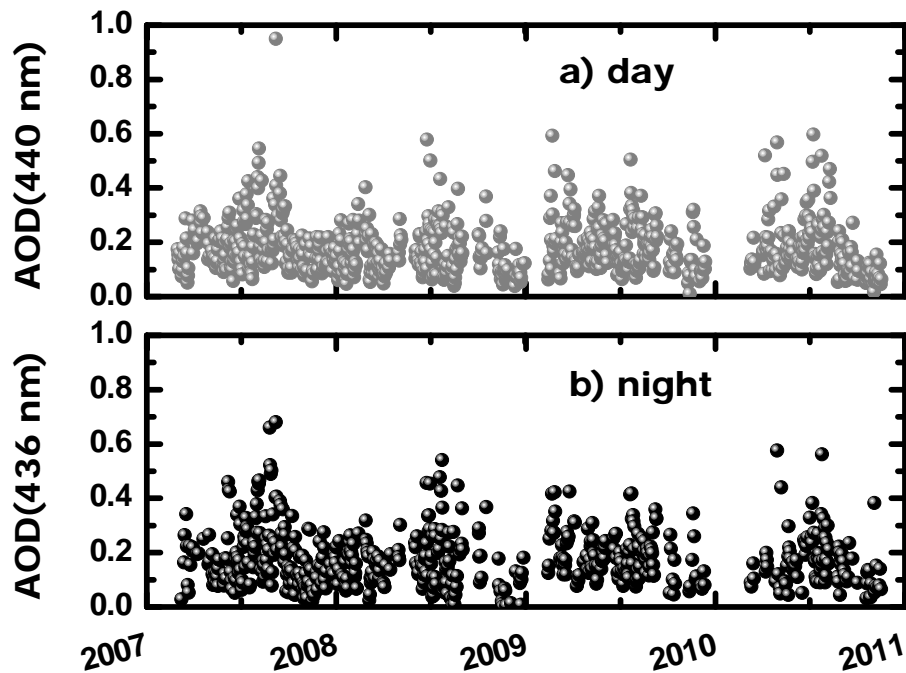


**Fig. 1.** Temporal evolutions of: **(a)** day-time mean values of aerosol optical depth at 440 nm and **(b)** night-time mean values of aerosol optical depth at 436 nm. All the measurements were acquired at Granada from 2007 to 2010.

**Day and night  
columnar aerosol  
properties**

D. Pérez-Ramírez et al.

Title Page

Abstract

Introduction

Conclusions

References

Tables

Figures

◀

▶

◀

▶

Back

Close

Full Screen / Esc

Printer-friendly Version

Interactive Discussion



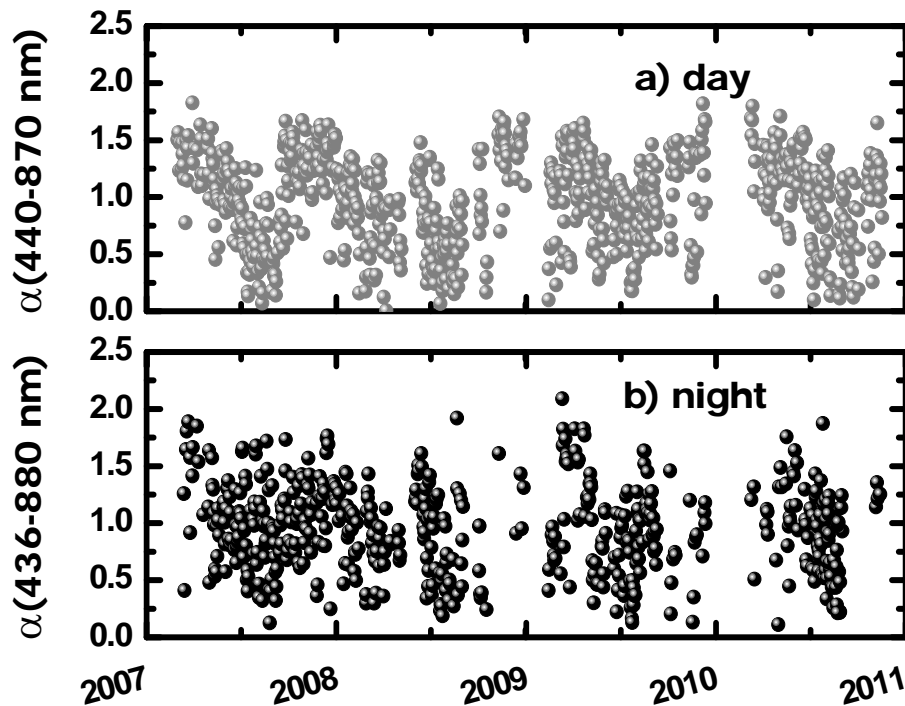


**Fig. 2.** Temporal evolutions of: (a) day-time mean values of the Angström exponent,  $\alpha$  (440–870 nm) and (b) night-time mean values of the Angström exponent,  $\alpha$  (436–880 nm). All the measurements were acquired at Granada from 2007 to 2010.

**Day and night  
columnar aerosol  
properties**

D. Pérez-Ramírez et al.

Title Page

Abstract

Introduction

Conclusions

References

Tables

Figures

◀

▶

◀

▶

Back

Close

Full Screen / Esc

Printer-friendly Version

Interactive Discussion



Day and night  
columnar aerosol  
properties

D. Pérez-Ramírez et al.

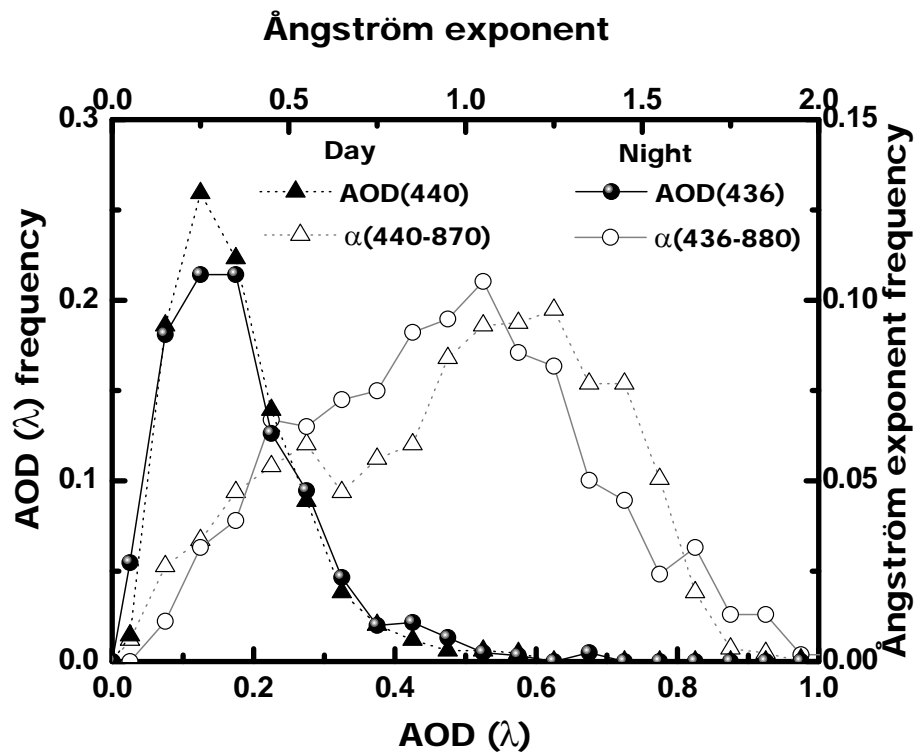


**Fig. 3.** Frequency histograms of AOD(440 nm) and  $\alpha(440-870)$  obtained at day-time and of AOD(436 nm) and  $\alpha(436-880)$  obtained at night-time for the period 2007–2010.

[Title Page](#)[Abstract](#)[Introduction](#)[Conclusions](#)[References](#)[Tables](#)[Figures](#)[◀](#)[▶](#)[◀](#)[▶](#)[Back](#)[Close](#)[Full Screen / Esc](#)[Printer-friendly Version](#)[Interactive Discussion](#)

## Day and night columnar aerosol properties

D. Pérez-Ramírez et al.

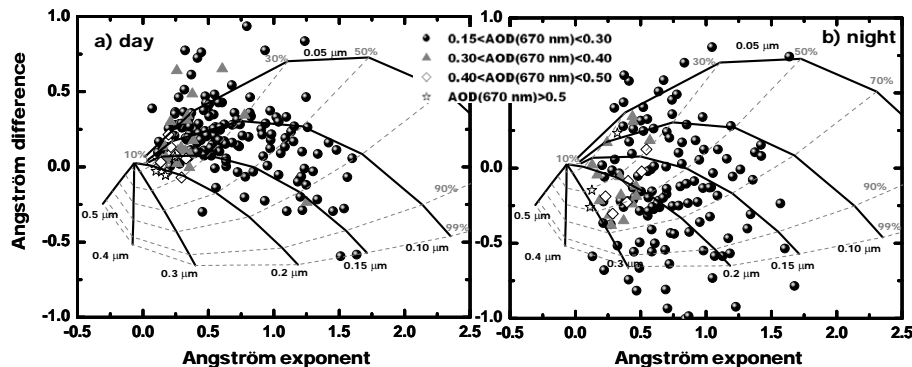


**Fig. 4.** (a) Angström exponent difference  $\delta\alpha = \alpha(440\text{--}670\text{ nm}) - \alpha(670\text{--}870\text{ nm})$  as function of  $\alpha(440\text{--}870\text{ nm})$  at day and (b) Angström exponent difference  $\delta\alpha = \alpha(436\text{--}670\text{ nm}) - \alpha(670\text{--}880\text{ nm})$  as function of  $\alpha(436\text{--}880\text{ nm})$  at night-time. Both  $\delta\alpha$  and the Angström exponents are the mean day or night values for the period 2007–2010. Different symbols indicate the ranges of aerosol optical depth at 670 nm used.

Title Page

Abstract

Introduction

Conclusions

References

Tables

Figures

◀

▶

◀

▶

Back

Close

Full Screen / Esc

Printer-friendly Version

Interactive Discussion



## Day and night columnar aerosol properties

D. Pérez-Ramírez et al.

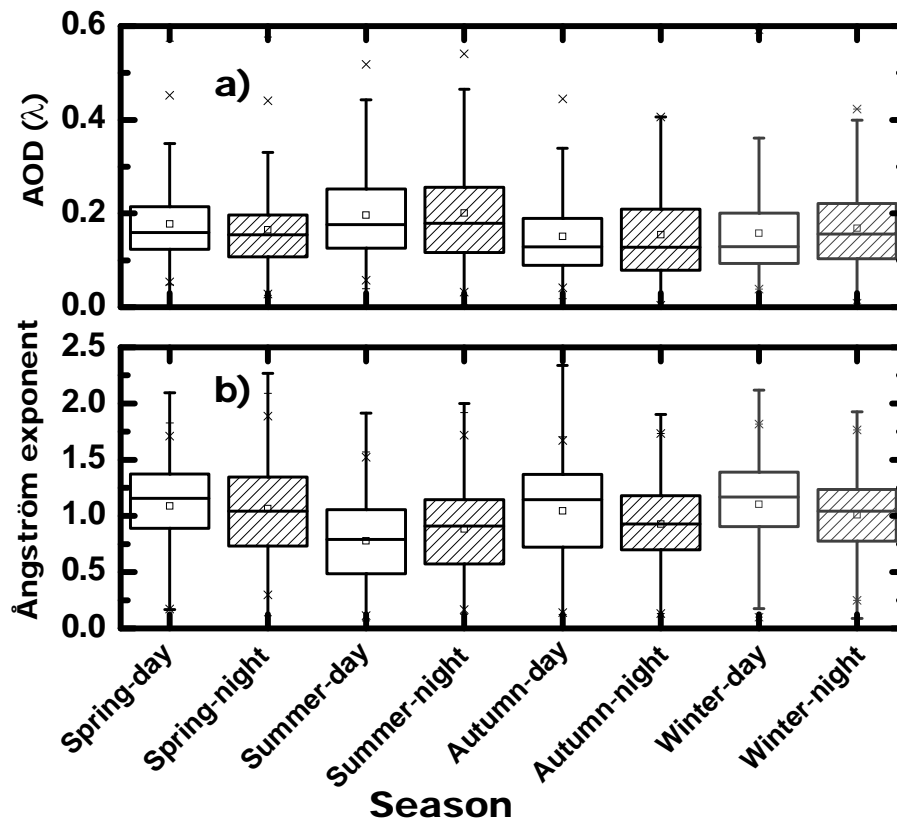


**Fig. 5.** Seasonal Box-Whisker diagrams of (a) AOD(440 nm) and AOD(436 nm) (b)  $\alpha(440\text{--}870\text{ nm})$  and  $\alpha(436\text{--}880\text{ nm})$  obtained at day and night time, respectively, during the period from 2007 to 2010. Dashed Box is for night-time data and empty Box is for day-time data.

[Title Page](#)
[Abstract](#)
[Introduction](#)
[Conclusions](#)
[References](#)
[Tables](#)
[Figures](#)
[Back](#)
[Close](#)
[Full Screen / Esc](#)
[Printer-friendly Version](#)
[Interactive Discussion](#)

## Day and night columnar aerosol properties

D. Pérez-Ramírez et al.

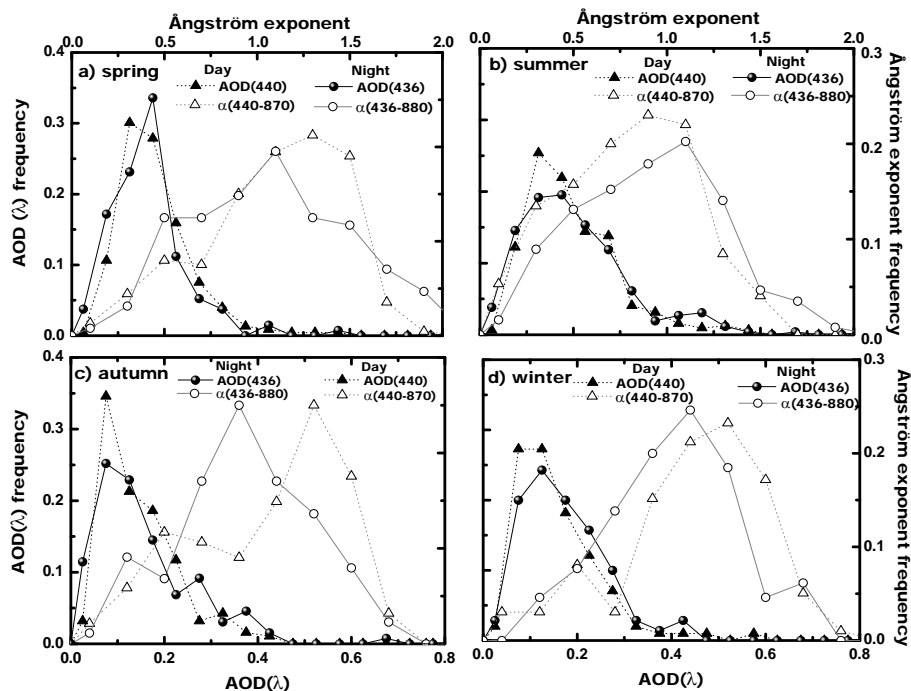


**Fig. 6.** Frequency histograms of AOD(440 nm) and  $\alpha(440\text{--}870\text{ nm})$  obtained at day time and of AOD(436 nm) and  $\alpha(436\text{--}880\text{ nm})$  obtained at night time for: **(a)** spring **(b)** summer **(c)** autumn **(d)** winter.

[Title Page](#)
[Abstract](#)
[Introduction](#)
[Conclusions](#)
[References](#)
[Tables](#)
[Figures](#)
[◀](#)
[▶](#)
[◀](#)
[▶](#)
[Back](#)
[Close](#)
[Full Screen / Esc](#)
[Printer-friendly Version](#)
[Interactive Discussion](#)


## Day and night columnar aerosol properties

D. Pérez-Ramírez et al.

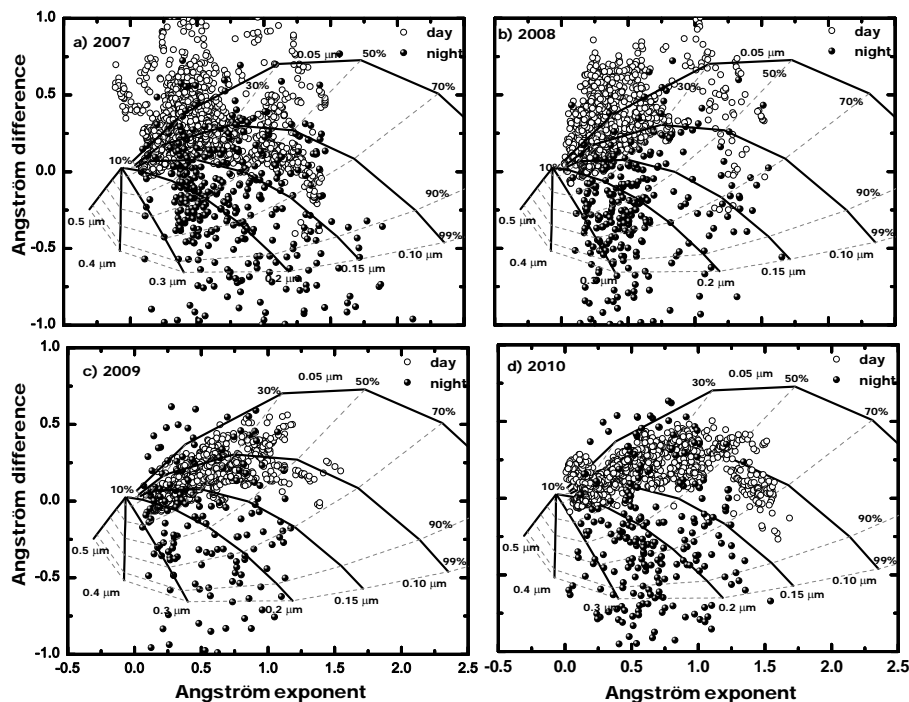


**Fig. 7.** Angström exponent difference  $\delta\alpha = \alpha(440\text{--}670\text{ nm}) - \alpha(670\text{--}870\text{ nm})$  as function of  $\alpha(440\text{--}870\text{ nm})$  at day and  $\delta\alpha = \alpha(436\text{--}670\text{ nm}) - \alpha(670\text{--}880\text{ nm})$  as function of  $\alpha(436\text{--}880\text{ nm})$  at night-time, for summer season. **(a)** For year 2007. **(b)** For year 2008. **(c)** For year 2009. **(d)** For year 2010. Each point presented in that figure corresponds to a single measurement with sun-photometry or 30 min average measurements with star-photometry.

[Title Page](#)
[Abstract](#)
[Introduction](#)
[Conclusions](#)
[References](#)
[Tables](#)
[Figures](#)
[◀](#)
[▶](#)
[◀](#)
[▶](#)
[Back](#)
[Close](#)
[Full Screen / Esc](#)
[Printer-friendly Version](#)
[Interactive Discussion](#)

## Day and night columnar aerosol properties

D. Pérez-Ramírez et al.

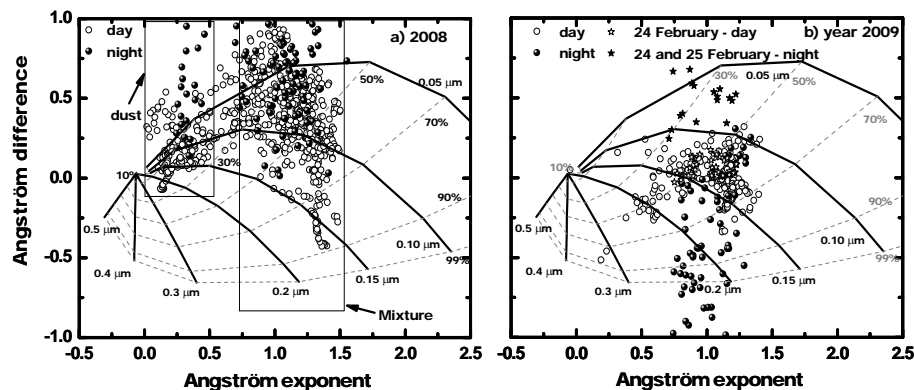


**Fig. 8.** Angström exponent difference  $\delta\alpha = \alpha(440\text{--}670\text{ nm}) - \alpha(670\text{--}870\text{ nm})$  as function of  $\alpha(440\text{--}870\text{ nm})$  at day and  $\delta\alpha = \alpha(436\text{--}670\text{ nm}) - \alpha(670\text{--}880\text{ nm})$  as function of  $\alpha(436\text{--}880\text{ nm})$  at night-time, for the winter season. **(a)** For year 2008. **(b)** For year 2009. Each point presented in that figure corresponds to a single measurement with sun-photometry or 30 min average measurements with star-photometry.

Title Page

Abstract

Introduction

Conclusions

References

Tables

Figures

◀

▶

◀

▶

Back

Close

Full Screen / Esc

Printer-friendly Version

Interactive Discussion

